A BRDF-RELATED BRIGHTNESS GRADIENT IN AVIRIS IMAGERY: LESSONS FROM AN EMPIRICAL COMPENSATION METHOD

Robert E. Kennedy*, Warren B. Cohen**, and Gen Takao***

1. INTRODUCTION

1.1 Goal of this paper

A brightness gradient was observed in the cross-track dimension of 1994 AVIRIS imagery acquired over a densely-forested study area in Oregon's Cascade Mountains. To compensate for the effect, Kennedy et al. (1997) tested four empirical methods based on simple quadratic fitting of the gradient. Interpretation of the fitting coefficients suggested that the gradient was caused primarily by vegetative bidirectional reflectance characteristics. In this paper, we discuss how the character of the brightness gradient may affect common analysis techniques of AVIRIS imagery such as classification, multi-image matching, and endmember selection.

1.2 Extent of problem

The 1994 AVIRIS imagery under study was collected with the aircraft heading nearly perpendicular to the solar plane, causing the scanning plane to closely parallel to the plane of the sun. These conditions accentuate bidirectional reflectance effects (Ranson et al, 1994) which Kennedy et al. (1997) suggested were the primary determinant of the brightness gradient. In an attempt to minimize the brightness gradient, 1996 AVIRIS images were collected with aircraft heading nearly parallel with the solar plane. Nevertheless, preliminary analysis showed that the effect was still present in the 1996 imagery (data not shown). The brightness gradient has also been reported in AVIRIS imagery at Harvard Forest, another densely-forested study area (Steve Newman, University of New Hampshire, personal comm.). Solar plane was slightly west of aircraft heading in one image and slightly east of aircraft heading in a second image, and the directional trend of the brightness gradient was reversed in the two images. The co-occurence of dense forests and the brightness gradient suggests that the effect may be an issue at other forested sites; the observance of the brightness gradient under a wide variety of sun-viewer geometries suggests the effect may occur with most flights at such sites and may be sensitive to solar position.

1.3 Interpretation of brightness gradient

The brightness gradient can be conceptualized as follows:

$$v(\alpha,\lambda) = [b \times f_{type}(\alpha,\lambda)] + C_{type}(\alpha,\lambda) \qquad \text{(Eq. 1)}$$

where $v(\alpha,y)$ is the brightness effect for a pixel at view-angle α and wavelength λ, b is some measure of that pixel's inherent brightness, f_{type} is a function describing the response to changes in view-angle for surface type equal to *type* at view-angle α and wavelength λ, and C_{type} is the additive function of view-angle effect for *type* and waveband λ (adapted from Kennedy et al., 1997).

The determinants of both $f_{type}(\alpha)$ and $C_{type}(\alpha)$ include the structure and physical features of the surface, the viewing geometry of the sun-surface-sensor configuration, and potentially atmospheric BRDF effects. The nature of the brightness gradient in the 1994 AVIRIS imagery utilized in this study suggested

* Department of Forest Science, Oregon State University, Forestry Sciences Laboratory, Corvallis, OR
** USDA Forest Service, Pacific Northwest Research Stations, Forestry Sciences Laboratory, Corvallis, OR
*** Remote Sensing Laboratory, Forestry and Forest Products Research Institute, Ministry of Agriculture, Forestry, and Fisheries, Tsukaba, Japan

that the majority of the effect was related to the surface bidirectional effects of vegetation, not by atmospheric effects (Kennedy et al., 1997).

2. METHODS

2.1 Image processing and brightness gradient compensation

The image processing techniques are described in Kennedy et al. (1997). The AVIRIS image was acquired on July 19, 1994. Aircraft heading was nearly perpendicular to solar azimuth. ATREM (Gao et al., 1993) was used to convert radiance to apparent surface reflectance.

The brightness gradient compensation method used in this paper is the "multiplicative-classified" approach of Kennedy et al. (1997). Of the four methods tested, the multiplicative-classified technique appeared to best preserve spectral integrity of the data. The compensation process modeled $f_{type}(\alpha)$ and $C_{type}(\alpha)$ as a single quadratic equation (Brown et al., 1982; Leckie, 1987), and used a pixel's initial reflectance as an estimate for b, using three "BRDF" classes (see Kennedy et al., 1997 for a description of the classes).

2.2 Other processing techniques

To explore whether common AVIRIS imagery analysis techniques may be affected by the presence of a view-angle-related brightness gradient, we conducted two processing routines on the 1994 AVIRIS data.

The first exploratory routine was a comparison of spectral classifications before and after brightness-gradient compensation. A maximum likelihood classifier was used to partition each 154-band image into 20 classes. No ground data were used to ground-truth these classes. Instead, patterns in these classes were compared visually with an independently-derived and ground-truthed classification based on Landsat Thematic-Mapper (TM) data (Cohen et al., 1995).

The second exploratory routine was designed to understand how the character of a relatively stable spectral class could change as view-angle changed under brightness-gradient conditions. For the purposes of illustration, the spectral class ideally would be derived from an independent source unaffected by the brightness gradient. We used a TM-based image of percent conifer forest cover (Cohen et al., *In prep.)*. This image (separate from the TM-based classification used in the first exploratory routine) was independently ground-truthed, with an r^2 of prediction of 0.76. From this image, pixels with 99 or 100% conifer were chosen as a nearly-pure conifer-class, and their average reflectance by wavelength across scan angles for all spectral bands was calculated in the manner of Kennedy et al. (1997).

3. RESULTS

3.1 Classification

Classification appears to be influenced by the presence of the brightness gradient. Figure 1 shows the maximum likelihood classifications of the AVIRIS image before and after brightness-gradient compensation, with the TM-derived classification for comparison. To aid in interpretation and to lower visual confusion, the three darkest and the three brightest AVIRIS classes are lumped and displayed, and the 14 intermediate classes are omitted from the figure. Similarly, the TM classes roughly corresponding to the AVIRIS bright and dark lumped classes are displayed in the same tones, and the intermediate TM classes are omitted from the figure. Following the terminology of Cohen et al. (1995), the bright class displayed in Figure 1c as gray pixels corresponds to Open (0-30% mixed conifer and broadleaf cover) and Semi-open (30-85% mixed conifer and broadleaf cover) classes, and the dark class displayed as black pixels is Old-growth conifer (>85% old-conifer forest cover). The TM classes are not meant to correspond

in a one-to-one fashion with the AVIRIS unsupervised classes, but rather to serve as a visual indicator of patterns of light and dark classes on the landscape.

The distribution of bright and dark classes were quite different in the pre- and post-compensation AVIRIS classifications. In the pre-compensation AVIRIS classification, most of the dark class pixels were at the bottom half of the image (on the forward-scatter side of nadir) and few were in the top half of the image. The converse was true for the light class. In the post-compensation AVIRIS classification, the two classes were fairly evenly distributed between the top and bottom half of the image. The patterns of bright and dark classes displayed in the TM classification indicate that bright and dark classes are fairly evenly distributed across the landscape, suggesting that the post-compensation image more accurately reflects the patterning of classes on the landscape.

3.2. Changes in spectral class across view-angles

The character of the conifer forest class was also affected by the brightness gradient. Figure 2 shows the average reflectance for pixels in this class across scan angles. In order to illustrate the trend associated with scan angle, groups of 20 adjacent scan columns were lumped before display (Figure 2a). Because of misregistration errors and differing sensor characteristics between AVIRIS and TM, there is significant variability in the reflectances of these pixels across scan angles. Nevertheless, it is evident that the general trend is toward brighter pixels on the back-scatter side of nadir and darker pixels on the forward-scatter side of nadir. Figure 2b shows the ratio between the spectral reflectances of the scan angle furthest on the backscatter side to the scan angle furthest on the forward-scatter side of nadir. Not only is the backscatter spectrum as much as two and half-times as bright as the forward-scatter spectrum, but the ratio changes with wavelength.

The trend with scan angle in this class was consistent with trends observed in vegetative BRDF classes in Kennedy et al. (1997). Maximum reflectance for any given waveband was found at the scan angle furthest from nadir in the backscatter direction. Minimum reflectance was found at a point offset from nadir slightly in the forward-scatter direction.

4. DISCUSSION

4.1 Evaluating these examples

Neither example presented here was without potential problems. In the classification example, it was only certain that the pre- and post-classifications were different, not that one was better. It appeared that the post-compensation classification better represented the TM-image classification, but because of the different sensor types and the different years of acquisition, there can be no certainty. Similarly, the correspondence of TM-derived conifer pixels to spectra observed in AVIRIS imagery is not perfect, and thus the conifer class as tested likely included pixels from other classes. Additionally, the predicted conifer results in the TM scene, although good, were not perfect, further adding error. Finally, the compensation method itself was only designed a compensation, not a correction. There is error and miscompensation in the technique. A simple empirical technique cannot account for the infinite complexity of surface BRDF effects in a scene.

Despite their weaknesses, the results presented here strongly suggest that the brightness gradient could have an effect on many basic analyses of AVIRIS imagery. Classification techniques make use of variability in spectral space to determine placement of similar pixels into classes. They assume that pixels in a given class will have similar reflectance anywhere in the scene and that they will differ from other classes anywhere in the scene. The brightness gradient function modifies reflectance based on view-angle ($v(\alpha,\lambda)$), thus nullifying these latter assumptions by introducing a spatial component to the spectral variability. By extension, any technique that assumes that variation in spectral space is unrelated to position in the scene will be affected by the brightness gradient.

Similarly, any technique that uses spectral reflectance to predict a continuous variable will be affected by the brightness gradient. Although the conifer pixels used in the above example contained natural variability, it was evident that, on average, pixels with high percent coverage by conifer forest displayed a trend related solely to scan angle. A relationship between percent conifer coverage and spectral reflectance developed at one scan angle would provide erroneous values most other scan angles. Similarly, spectral unmixing would be affected. The spectral variability introduced by the view-angle-effect would be translated into variability in fractions of endmembers, thus introducing error that would be based solely on scan angle.

4.2 Other affected image-processing techniques

The other major category of processing technique that would be affected by the brightness gradient would be multi-image comparisons. An obvious example would be comparing two images acquired over the same site, but with the aircraft heading in the second image rotated 90 degrees relative to the heading in the first image. The overlay of perpendicular brightness gradients would introduce significant spectral artifacts that would need to be accounted for before change detection could take place. Similarly, two scenes flown at the same heading, but imaged under different sun angle conditions, would be affected, especially if the sun moves to opposite side of nadir (e.g. the example from Harvard Forest described in Section 1.2). Finally, mosaicking images from adjacent flight lines would show an extremely pronounced image seam, since the overlap area would be on the backscatter side of nadir in one flightline and the forward-scatter side of nadir in the other.

4.3 Some potentially unaffected techniques

In the course of analysis, Kennedy et al. (1997) determined that spectral first derivative (Martin et al, 1994) was relatively unaffected by the compensation techniques. By inference, the first derivative image was apparently little affected by the brightness gradient. Because the first derivative as used by Martin et al (1994) relies on differences between adjacent bands, this resilience is likely explained by the fact that the change in brightness gradient from one band to the next at the same scan angle is relatively slight. Hence, analysis techniques that rely solely on first-derivative images may be little affected. Also, the ATREM procedure appeared to be relatively unaffected by the gradient. Kennedy et al. (1997) found that the same final image resulted when ATREM was run before view-angle compensation and when ATREM was run after view-angle compensation.

5. CONCLUSION

The exploratory examples presented here suggest that the view-angle-dependent brightness gradient evident in several AVIRIS images may affect spectral analysis. Analyses that may be affected are those that use some measure of scene-wide variability to predict or derive relationships: classification, unmixing, continuous variable prediction, etc. The gradient would manifest itself as increased variation unexplained solely by surface type. The problem existed in two years of imagery acquired for dense conifer forest of Oregon and existed in images from the mixed hardwood-deciduous forest of New England, and appeared to exist at a wide range of sun-object-viewer geometries. This suggests that other forested or densely vegetated systems may experience similar effects, and attention must be paid to this effect before analyses are conducted that rely on scene-wide measures of spectral variability.

References

Brown, R.J., Bernier, M.., and G. Fedosojevs, 1982, "Geometrical and atmospheric considerations of NOAA AVHRR imagery," In 1982 Machine Processing of Remotely Sensed Data Symposium, Purdue University Press, West Lafayette, IN, pp. 374-381.

Cohen, W.B., Spies, T.A., and M. Fiorella, 1995, "Estimating the age and structure of forests in a multi-ownership landscape of western Oregon, U.S.A.," Remote Sens. Env., vol. 16, no. 4, pp. 721-746.

Cohen, W.B., Maiersperger, T., Spies, T., and D.R. Oetter, *In Prep.*, "Continuous modeling of forest attributes across several Landsat TM images in western Oregon, U.S.A.."

Gao, B.-C., Heidebrecht, K.A., and A.F.H. Goetz, 1993, "Derivation of scaled surface reflectance from AVIRIS data," Remote Sens. Env., vol. 44, no. 2, pp. 165-178.

Kennedy, R.E., Cohen, W.B., and G. Takao, 1997, "Empirical methods to compensate for a view-angle-dependent brightness gradient in AVIRIS imagery," Remote Sens. Env., vol 62, pp. 277-291.

Leckie, D.G., 1987, "Factors affecting defoliation assessment using airborne multispectral scanner data," Photogramm. Eng. Remote Sens., vol. 53, no. 12, pp. 1665-1674.

Ranson, K.J., Irons, J.R., and D.L. Williams, 1994, "Multi-spectral bidirectional reflectance of northern forest canopies with the advanced solid-state array spectroradiometer (ASAS)," Remote Sens. Env, vol. 47, pp. 276-289.

Figure 1.
Comparison of 20-class maximum likelihood unsupervised classification of AVIRIS data a) before and b) after view-angle compenation. The three darkest spectral classes are portrayed in black; the three brightest in grey. All intermediate classes in white. The nadir line runs horizontally across the middle of these two images.
c) For comparison, an independent, ground-truthed, TM-based classification for the same area (Cohen et al., 1995). Classes with 0 to 85% cover in the mixed forest category are displayed in gray; classes in the old-conifer category (>200 yrs.) are displayed in black. The post-compensation AVIRIS classification better mimics the distribution of bright and dark classes observed in the independent TM classification.

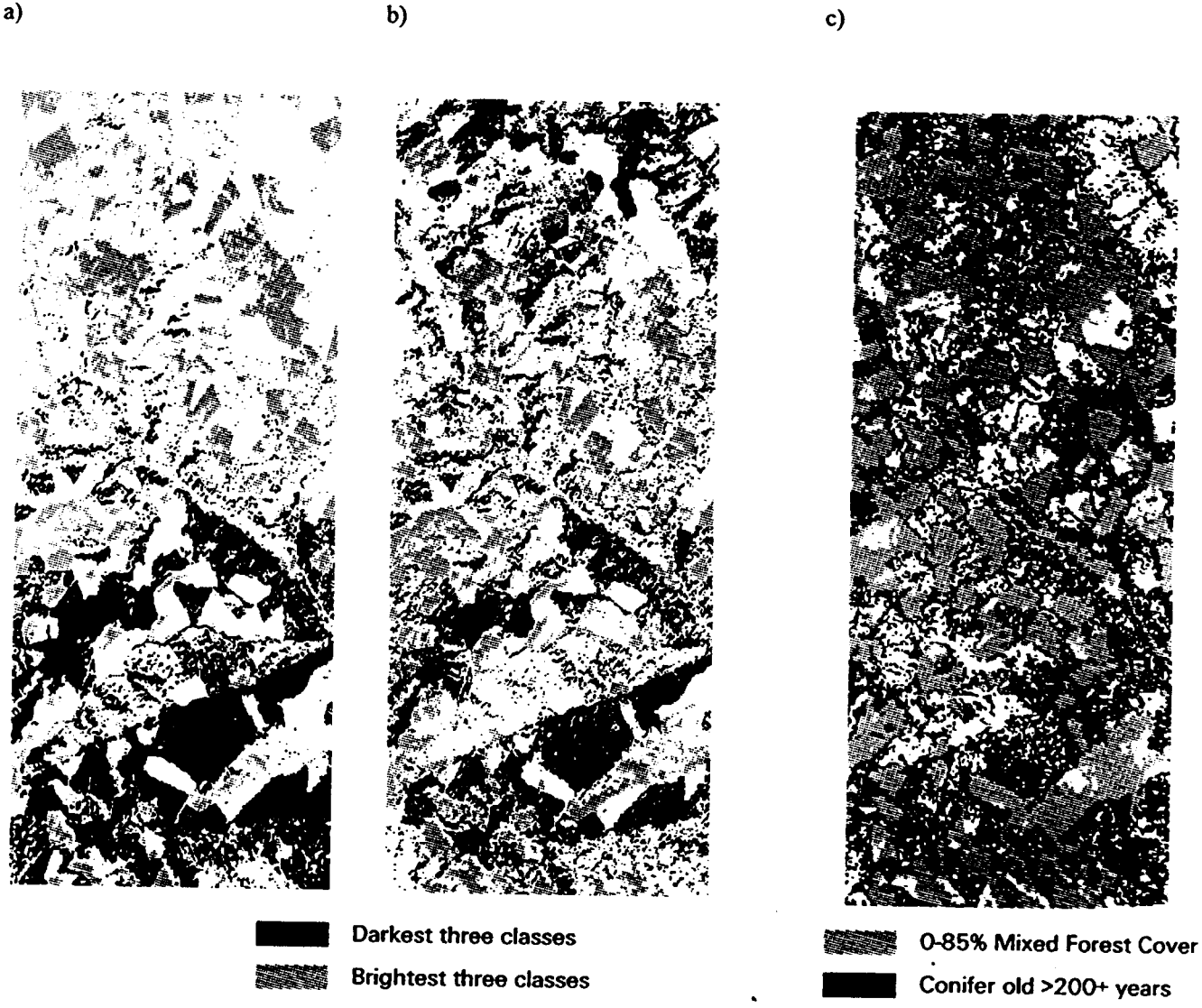

a)

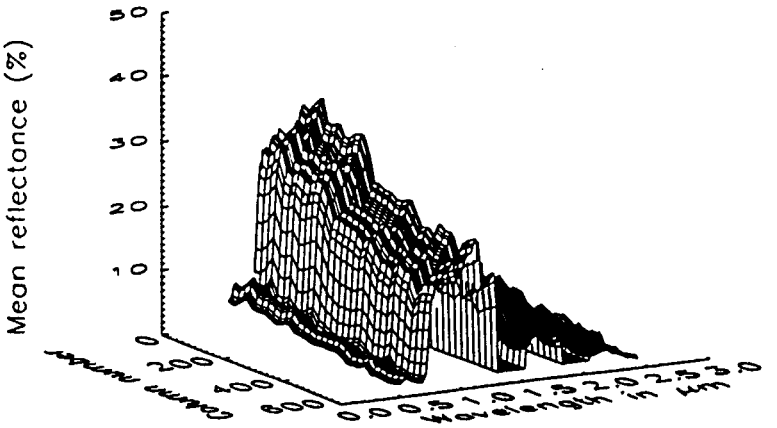

b)

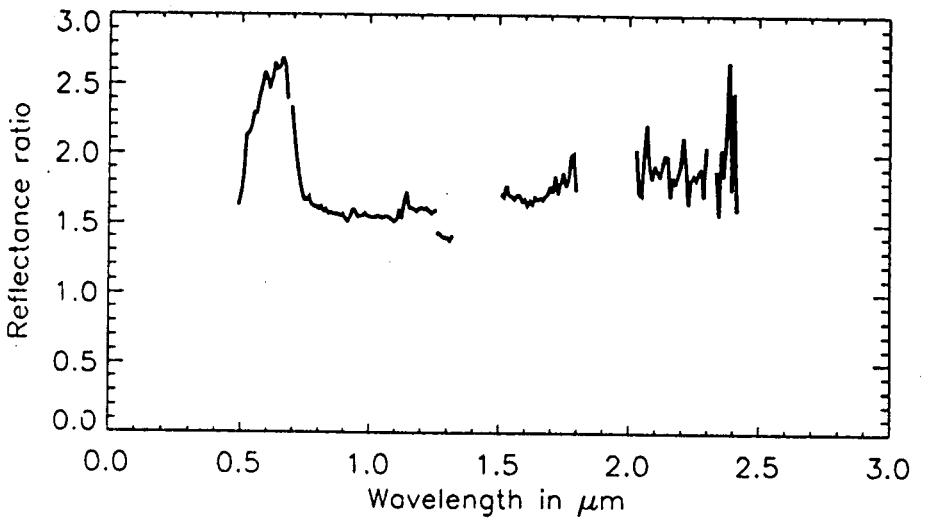

Figure 2. a) Average spectral reflectance of 99 and 100% conifer forest cover pixels across view-angles. Column number follows view-angle; nadir view is at column 306. b) The ratio of spectral reflectance of column 1 over column 614.